DOI: 10.13009/EUCASS2019-751

8TH EUROPEAN CONFERENCE FOR AERONAUTICS AND AEROSPACE SCIENCES (EUCASS)

DOI: ADD DOINUMBER HERE

Absolute and Convective Instabilities in High Enthalpy Jets

S. Demange[1] *and F. Pinna*[2]
von Karman Institute for fluid dynamics
Rhode-Saint-Genese, Belgium
simon.demange@vki.ac.be · fabio.pinna@vki.ac.be

Abstract

The full impulse response of the high enthalpy axisymmetric jet of the VKI plasma wind tunnel Plasmatron is investigated using the Linear Stability Theory. Results show that the jet is absolutely unstable for all conditions studied. A parametric study shows the dependency of the absolute region on the coaxial nature of the jet. A competition mechanism between convective shear layer and absolute jet column modes is revealed by varying the group velocity of the wave packet. Results are compared against available experimental observations, matching the trends observed and a possible explanation for the mismatch in the frequency range is proposed.

1. Introduction

Understanding and predicting physical phenomena occurring during the atmospheric entry of manned capsules is still one of the most challenging issue of present day space exploration. Due to high orbital velocities, the air in front of the objects approaching the earth is compressed, forming a bow shock through which pressure and temperature increase drastically until the air dissociates and reaches a state in which the gases are ionized called plasma. To study such high enthalpy flows, the Von Karman Institute operates since 1997 the most powerful Inductively Coupled Plasma wind tunnel in the world:[4] the Plasmatron. However, the phenomena studied in this facility, such as the ablation of Thermal Protection System materials and flow transition, are strongly coupled with the quality of the plasma jet blown into the test chamber, and the reproduction of conditions similar to atmospheric entry in the facility is eventually hampered by hydrodynamic instabilities of the jet. The experimental campaign of Cipullo et al.[7] highlighted the leading the leading role of the facility's static pressure on the frequency behavior of the jet's oscillations using high speed camera recordings, however without providing a physical interpretation of the oscillations mechanism.

Since the observations of "irregular" instability modes in inviscid jets by Michalke[19] in 1984, the concept of absolute instability has become an important aspect of stability studies in shear flows. Formally introduced by Huerre and Monkewitz[13] for open shear layers, absolute instabilities have been found to promote self-sustained oscillations in heated jets depending on flow parameters, first theoretically by Monkewitz and Sohn[21] and later experimentally by Monkewitz.[22] Huerre and Monkewitz[13] also adapted the Briggs-Bers geometric criterion used to determine the absolute/convective nature of instabilities in plasma physics from the work of Briggs[5] and Bers[3] to continuous flows. Literature has since shown the relevance of using the spatio-temporal formulation of the Linear Stability Theory (LST), assuming perturbations growing both in time and space, for absolutely unstable flows.

Whether to promote mixing or stabilize shear layers, the influence of flow parameters on the changeover from convective to absolute instabilities has been extensively studied in the literature. Monkewitz and Sohn[21] showed that absolute instability arises in jets with a density ratio under $S_e = \rho_c/\rho_\infty = 0.72$ at the nozzle exit. However, this ratio could be decreased by either increasing the Mach or the azimuthal mode numbers, or by decreasing the velocity ratio. Lesshafft and Huerre[17] later confirmed the damping effect of increasing the Mach number, and added that delaying the change from convective to absolute instabilities could also be obtained by lowering the Reynold's number. They furthermore highlighted the competition mechanism between absolute jet-column modes and convective shear layer modes for different group velocities fo the perturbations by considering the full impulse response of the flow. Balestra et al.[1] extended this analysis to more complex coaxial heated jets, for which two absolutely unstable modes appeared respectively in the inner and outer shear layers. Outer modes proved to promote absolutely instabilities for higher density ratios than the values met in single jets, although reaching smaller amplification when compared to the inner modes. This study was however limited to cases where only the inner shear was heated and where both shear layers had the same thickness. Coenen et al.[8] brought additional results for more realistic jet profiles based on boundary layer equations, and compared the frequency of locale absolute instability to the one of global modes. Studies of the

DOI: 10.13009/EUCASS2019-751

effect of confinement carried out by Juniper[14] found it to also promote absolute instabilities. This study also brought a more complete methodology for the identifications of valid saddle points in the complex wave-number plane used to apply the Briggs-Bers criterion. Similarly to absolute instabilities, increasing the viscosity and the Mach number was found to have a stabilizing effect on convective instabilities by Gloor et al.[11] for coaxial jets.However, to the author's knowledge, all previous studies of absolute instabilities relied on the Calorically Perfect Gases (CPG) model and profiles shapes far from the one met in the Plasmatron jet.
The aim of this study is to compute the spatio-temporal impulse response of the Plasmatron jet for several stream-wise positions and input parameters of the facility, to uncover the nature of the instabilities observed and compare these results against experimental observations.
This paper is organized as follow: Section 2 introduces the methods used to obtain the base flow from high-enthalpy CFD simulations and the theory used for the stability study. A brief description of the numerical methods is given in section 2.3. Section 3 presents the results obtained. At first, the influence of Plasmatron's driving parameters on the basic state is discussed in term of non-dimensional numbers and flow parameters in Section 3.1. Then the full impulse response is studied in Section 3.2. The nature of the instabilities is investigated along the test chamber in Section 3.3, and for the different driving parameters of the facility in Section 3.4. Section 3.5 offers a comparison against experimental observations. Finally, section 4 presents the conclusions of the study.

2. Problem and model description

2.1 Base flow

The geometry investigated in the present work represents the torch and partial test chamber sections of VKI plasma wind tunnel Plasmatron, assumed to be perfectly axi-symmetric. The cylindrical co-ordinates (z, r, θ) are respectively the stream-wise, radial and azimuthal directions, and the origin of the stream-wise position z is placed at the beginning of the torch section, and the chamber section starts at $z = 0.486$ m. To generate the plasma jet, the test gas is blown through an annular inlet into the torch section, where it is heated up to ionization[4] by induction, and finally enters the test chamber forming a hot jet as seen in Figure 1. One should note that because the computational domain is smaller than the actual size of the facility, open boundary conditions are applied at the outlets locations of the test chamber.

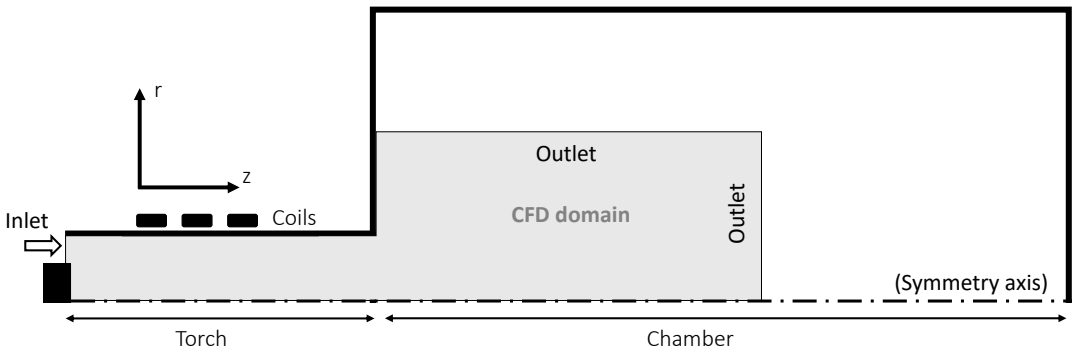

Figure 1: Sketch of the Plasmatron facility and CFD domain.

CFD simulations of the torch and partial test chamber are performed in the open-source Computational Object-Oriented Library for Fluid Dynamics CoolFluid-ICP[16] multi-physics numerical solver. No swirling of the jet is considered to match experimental conditions. Simulations are performed considering an eleven-species air mixture with [N, O, NO, N2, O2, N+, O+, NO+, N2+, O2+, e-], allowing for air ionization phenomena in equilibrium. The mixture is assumed to be in Local Thermo-chemical Equilibrium (LTE), which is close to experimental observations[7] considering static pressures in the chamber between 100 mbar and 200 mbar used in this study. Simulations call the MUlticomponent Thermodynamic And Transport properties for partially IONized gases in C++ Mutation++[25] library to compute the transport properties of the flow. Furthermore, buoyancy effects are neglected.
Nine cases summarized in Table 1 are considered for this study, and are defined by a combination of the following facility's driving parameters:

DOI: 10.13009/EUCASS2019-751

- $\dot{m}$: The inlet mass flow, kept constant to 16 g/s in this study;
- P_s: The static pressure, imposed at the outlet boundaries of the CFD domain, and kept in the range where the flow is in LTE;
- P_{el}: The power received by the plasma in CoolFluid-ICP. In practice, a ratio of ½ is assumed between the power given to the facility and the one set for the simulations. Estimating the efficiency of Plasmatron remains an open topic[9] and is currently under investigation.

As linearized stability equations involve up to the 2^{nd} order derivatives of the flow quantities with respect to the radial dimension, the MATLAB™ *fit* routine is used to interpolate the velocity and temperature profiles from the CFD simulations at discrete stream-wise positions using an analytical model detailed in the appendix section 5. The derivatives of the flow quantities are then computed analytically. However, the model does not guarantee a stream-wise continuity of the basic state, which can lead to small oscillations in the evolution of stability features along the test chamber. For the conditions studied, the local model introduces up to an overall error of 0.4% of the temperature and 0.15% of the velocity at the torch outlet centerline when compared against the CFD simulations, which is considered negligible. The thermodynamic and transport properties needed by the stability solver are then obtained using look-up tables of LTE properties for the chosen static pressure and temperature profile. The tables are generated using the Spectral Multi-Regime Basic-State Solver for Boundary-Layer Stability DEKAF,[12] as it proved to give smoother derivatives of the properties with respect to pressure and temperature than the ones numerically computed from Mutation++. More details about the property models and their influence on stability are available in the work[20] of F. Miro Miro. At each stream-wise position, the quantities are non-dimensionalized with respect to their centerline values denoted by the subscript "c", with the exception of the reference pressure defined as $\rho_c W_c^2$, and the main non-dimensional numbers involved in the stability equations are:

$$Re = \frac{\rho_c W_c r_0}{\mu_c} \quad , \quad Pr = \frac{\mu_c h_c}{\kappa_c T_c} \quad , \quad Ec = \frac{W_c^2}{h_c}. \tag{1}$$

Where the reference length $r_0 = 0.08$ m is the radius of the torch section, Re is the Reynold number, Pr is the Prandtl number and Ec is the Eckert number. The equilibrium quantities ρ_c, μ_c, κ_c and h_c are respectively the density, viscosity, thermal conductivity and static enthalpy obtained from DEKAF for the centerline value of the temperature T_c, while W_c is the stream-wise velocity at the centerline.

2.2 Linear Stability Theory

The stability features of the heated jets are investigated using the local Linear Stability Theory (LST). The stream-wise variations of the basic state are neglected, assuming a locally-parallel flow. The stability equations are obtained from the Navier-Stokes equations expressed in cylindrical co-ordinates. The state vector considered is [w, u, v, P, T], respectively the components of the velocity along (z, r, θ), the pressure and temperature. Flow quantities are decomposed into the sum of an averaged value and a small perturbation around this average: $q(z, r, \theta, t) = \bar{q}(z, r, \theta) + q'(z, r, \theta, t)$, with $q' \ll \bar{q}$. The absence of swirl in the jet and the parallel flow assumption impose respectively $\bar{v} = 0$ and $\bar{u} = 0$. Early stages of the transition to turbulence are considered, neglecting interactions between instabilities, therefore the physical perturbations can be modally decomposed:

$$q'(x, y, z, t) = \tilde{q}(r)\, e^{i(\alpha z + m\theta - \omega t)} + c.c. \tag{2}$$

Where α and q are respectively the stream-wise and azimuthal integral dimensionless wave-numbers, ω is the dimensionless frequency, $\tilde{q}(r)$ is the shape of the instability considered and $c.c.$ denote the complex conjugated. The dimensional frequency is retrieved from the real part of ω as $f = {}^{\omega_r W_c}/_{(2\pi r_0)}$. In the case where $q = 0$, the instabilities are axisymmetric. The compatibility conditions set at the centerline to cope with the co-ordinates singularity are detailed in the report[6] of Chiatto and depend on the value of the azimuthal integral wave-number q. As seen in Fig. 1, the CFD domain does not reach the physical outer wall of the test chamber, therefore the jet is considered as unconfined and the perturbations are assumed to vanish for $r \to \infty$.
By imposing either the wave-numbers or the frequency, the linearized stability equations and the appropriate set of boundary conditions reduce to an eigenvalue problem, also called *dispersion relation*, which encapsulate all the information of the normal instability modes for the basic state considered: $\mathfrak{D}(\omega, q, \alpha) = 0$. In this case, $\tilde{q}(r)$ is the eigenfunction associated with α, q and ω. The spatio-temporal formulation of the LST is used, imposing both α and ω to be complex numbers to consider waves growing both in time and space. The ensemble of solutions to the *dispersion relation* is called spectrum of instabilities, and the mode with largest growth-rate ω_i leads the stability behavior of the

DOI: 10.13009/EUCASS2019-751

flow.
A first set of linearized compressible Navier-Stokes equations in cylindrical coordinates has been developed at VKI by Garcia Rubio[10] and was later completed by Chiatto[6] to include high enthalpy effects. The latter is used in this study. In both cases, the electro-magnetic terms are neglected in the stability equations as their effects remain mostly confined to the torch section of the Plasmatron. Thermodynamic and transport properties perturbations are obtained from expansion of the base flow based on their derivatives with respect to pressure and temperature in LTE.
The absolute/convective nature of the instabilities is determined by the sign of the time asymptotic temporal growth rate of perturbations with nil group velocities $v_g = {}^{x}/_{t} = 0$ in the aftermath of a localized impulse. In other words, when an impulse excites self-sustained instabilities through a resonance mechanism in the flow. According to the Briggs-Bers criteria, this is similar to looking at the sign of the spatio-temporal growth rate where contours of the later form a saddle point in the complex wave-number plane (α_r, α_i). However, to respect the criteria, the saddle must be formed from by the pinching of an α^+ and an α^- branch, hence from the saddle point, contours of growing ω_i must reach respectively the $\alpha_i > 0$ and $\alpha_i < 0$ half-planes. The full impulse response of the flow is computed by varying the group velocity and tracking the evolution of the saddles in the α planes. The group velocity is varied using a similar technique than Lesshafft and Huerre,[17] by shifting the reference frame of the study.

2.3 Numerical methods

The implementation of the linearized equations was done by Chiatto[6] using the automatic derivation tool[24] in the framework of the VKI Extensive Stability and Transition Analysis toolkit VESTA[23] developed by Pinna. The stability equations reduced to an eigenvalue problem are also solved in VESTA, relying on the MATLAB^{TM} *eig* routine. The domain is mapped using Chebyshev collocation points in the radial direction, and further transformed using the tangential mapping technique developed by Bayliss and Turkel[2] as it proved well suited for problems with thick shear layers. A convergence study of the current cases showed that the values of the ω converged up to $1e-7$ for the current mapping and $N = 201$ collocation points.
Contours of the spatio-temporal growth-rate ω_i are obtained using a Newton's root finding algorithm to track a specific eigenvalue while complex values of the wave-number are swept. The position of saddle points are found using a Levenberg-Marquard-Fletcher least squares algorithm to find the roots of ${}^{\partial\omega}/_{\partial\alpha} = 0$. Finally, analytical tools developed by Kumar[15] to track saddle points in the parametric space have been adapted to the cylindrical co-ordinates numerical framework for the purpose of this study.

3. Results

3.1 Simulations of plasma jet

Fitted profiles of the stream-wise velocity, temperature and density of Plasmatron jet obtained for stream-wise positions through the test chamber are displayed figure 2 for a case where the electrical power is set to $P_{el} = 100$ kW and the static pressure to $P_s = 150$ mbar. For a better visibility, the density is normalized using its the outer flow in figure 2, although the stability equations are solved using the centerline value as reference. As seen from the velocity profiles, the flow forms a coaxial sharp jet near the exit of the torch section, due to the annular inlet and induction heating being mainly localized around the centerline. Around $z = 1.3$ m , the jet can no longer be considered coaxial, but rather display velocity and density profiles alike *top hat* jets with thick shear layers. Temperature profiles display humps characteristic from high temperature flows, due to the reactions occurring in the flow: around $T = 2500$ K the 0_2 starts to dissociate, then nitrogen around $T = 4000$ K, and finally the ionization starts around $T = 9000$ K.

The stream-wise evolution of the centerline velocity and temperature can be decomposed in two phases: Out of the torch exit both values decrease abruptly, reaching around 60% of their initial values before reaching $z = 1.25$ m for all cases. After this region, both the centerline velocity and temperature keep decreasing, but at a much lower rate. One can observe the effect of ionization on the flow viscosity, as the Reynolds number decreases until the temperature cools down under approximately $T = 9200$ K in all conditions studied. After this value, the Reynolds number increases until the end of the jet.
The evolution of the main flow parameters for the different cases studied is given in table 1, where the subscript "0" indicates a value taken at the centerline and at the exit of the torch ($z = 0.486$ m):

The initial Reynolds number is sensitive to both the static pressure P_s and the electrical power P_{el} of the facility. Increasing the pressure mainly decreases the core velocity at the torch exit, while almost not modifying the velocity of the secondary stream, therefore influencing the initial by-pass ratio h_0. Increasing the power also has a strong influence on the core and secondary stream velocities, while largely influencing the initial temperature as expected. Increasing

DOI: 10.13009/EUCASS2019-751

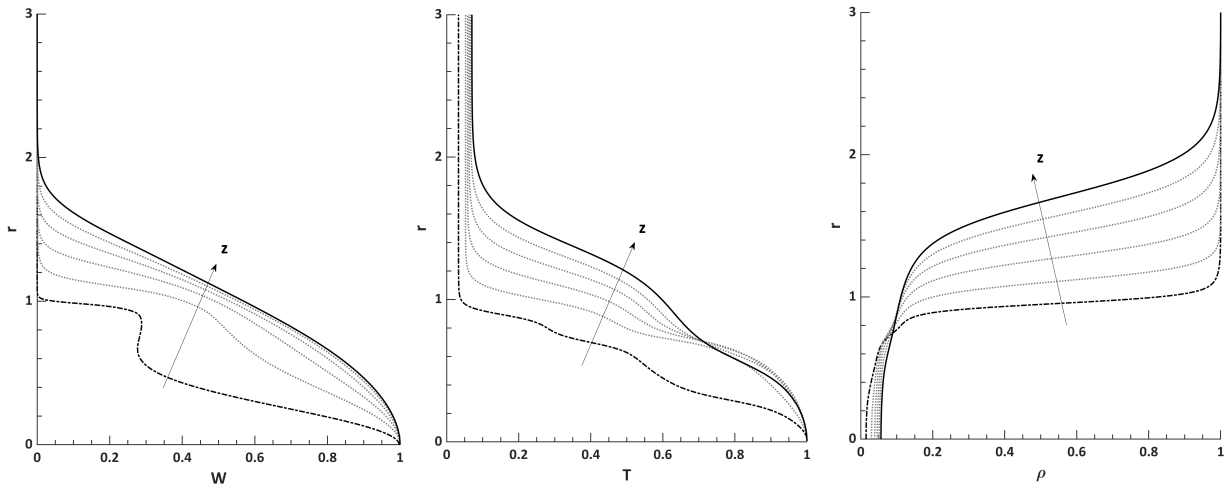

Figure 2: Fitted non-dimensional profiles of velocity (left), temperature (center) and density (right), from $z = 0.5$ m (- ·) to $z = 3$ m (-) for 100 kW and 150 kbar

P_{el} (kW)	P_s (mbar)	T_0 (K)	W_0 (m/s)	Re_0	S_0	M_0	h_0
80	100	10127	141.62	90.43	0.0345	0.0523	0.43
80	150	9829	103.54	95.90	0.0356	0.0391	0.39
80	200	9547	80.84	100.43	0.0366	0.0311	0.38
100	100	10711	196.65	130.25	0.0326	0.0690	0.32
100	150	10665	146.17	135.44	0.0328	0.0520	0.28
100	200	10549	117.10	138.63	0.0331	0.0422	0.26
150	100	11402	301.03	220.69	0.0306	0.0984	0.22
150	150	11387	230.24	229.35	0.0307	0.0766	0.19
150	200	11337	187.83	233.42	0.0308	0.0633	0.18

Table 1: Main non-dimensional numbers and parameters for the jets studied.

the power strongly decreases the the bypass ratio. Jets obtained for $P_{el} = 150$ kW show a much small area where the jet can be considered as coaxial when compared to $P_{el} = 80$ kW cases. The Mach number at the centerline is computed from the equilibrium speed of sound given by the Mutation++ library, and remains below 0.1 for all test conditions, therefore compressibility effects are believed to play a small role in the stability behavior of Plasmatron. One can note that the values of the temperature ratio S are one order of magnitude smaller than usual values found in the literature.

3.2 Full impulse response

3.2.1 Analysis for zero group velocity

A first temporal stability analysis is carried out for the case with $P_{el} = 100$ kW and $P_s = 150$ mbar, at the stream-wise position $z = 1.1$ m to identify the leading mode. The azimuthal integral wave-number is set to $q = 0$ based on the experimental observations of Cipullo et al.[7] As the recorded temperature perturbations seem to be non-zero at the centerline of the jet, the only compatible centerline boundary condition is the one for $q = 0$. Furthermore, stability computations considering non-zero azimuthal wave numbers yield smaller instability growth rate, which is in agreement with observation done by Lesshafft and Huerre[17] for heated top hat jets. A first spectrum of the instabilities obtained by imposing a real value of the stream-wise wave-number $\alpha = 1$ is displayed Fig. 3, allowing the identification of a single unstable temporal mode at this stream-wise position. This mode is found at $\omega = 0.11694 + 0.18348i$ for the current value of α and $N = 201$ discretization points. The eigen-vectors of the least stable mode are displayed figure 3, and the shapes correspond to the outer shear modes described by Gloor[11] and Balestra[1] in coaxial jets.

This mode is then tracked across the complex wave-number plane using the local solver to obtain the contours of constant spatio-temporal growth rate plotted figure 4. Several valid saddle points are identified over the wave-number plane, however only one of them is located above the $\omega_i = 0$ contour represented by a white slashed line in figure 4. This saddle is marked by a white circle figure 4 and is located at $\alpha_S = 0.46221 - 0.71639i$, its absolute growth-rate

DOI: 10.13009/EUCASS2019-751

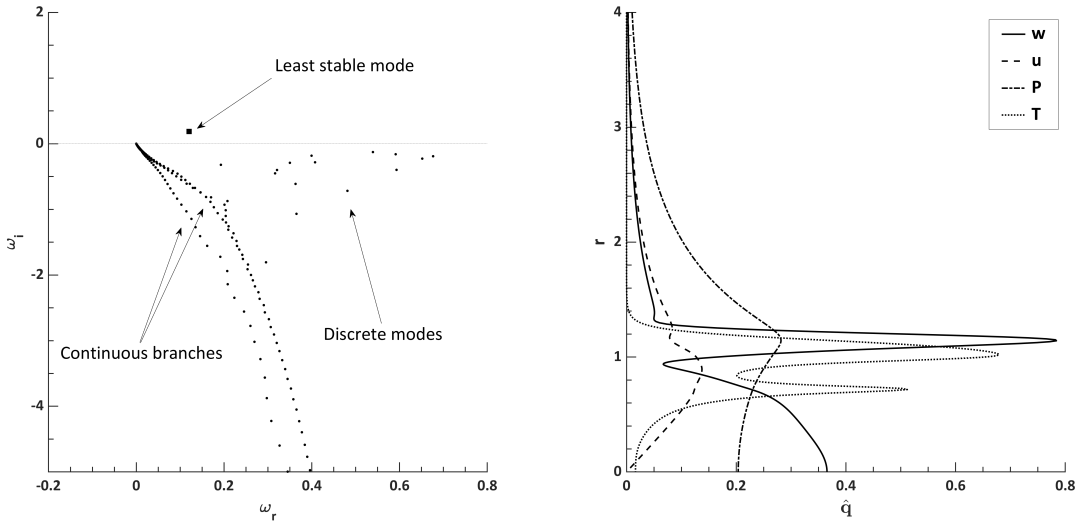

Figure 3: Spectrum of eigenvalues (left) and least stable mode perturbation shapes (right) obtained for $q = 0$ and $\alpha = 1$, at $z = 1.1$ m for the 100 kW and 150 mbar case using $N = 201$ Chebyshev points.

is $\sigma = \omega_{i,S} = 0.12186 > 0$ and absolute frequency $f_S = 24.5$ Hz. Therefore, the flow an be considered absolutely unstable. For all conditions studied, a similar saddle can be found, and is labelled S_1 for the rest of the study. The shape of the stream-wise velocity and pressure perturbations associated with S_1 are displayed figure 5, allowing to identify it as a mixed mode similar to the one observed by Balestra[1] in coaxial jets with vanishing bypass ratio $h \to 0$. Remaining saddles display lower absolute growth-rates and are therefore not considered. An additional saddle point can be found in the upper α plane, although not displayed here because pinched between two α^+ branches, and therefore not valid.

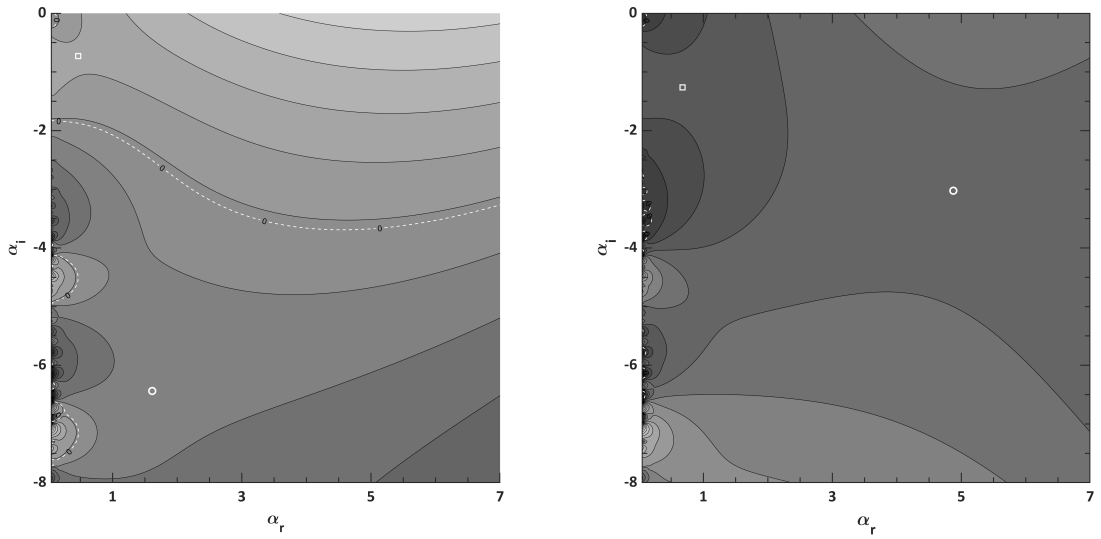

Figure 4: Contours of constant growth-rate ω_i in the complex wave-number plane α for $vg = 0$ (left) and $vg = 0.1$ (right) for the 100 kW and 150 kbar case at the $z = 3$ m position. Saddle S_1 and S_2 are respectfully indicated by a white square and circle.

DOI: 10.13009/EUCASS2019-751

3.2.2 Influence of the group velocity

Similarly to the study of Lesshafft and Huerre,[17] the full impulse response is considered by varying the group velocity. The group velocity value v_g is imposed by shifting the reference frame of the study, which is equivalent to shifting the velocity profiles:$W_{adim}(v_g) = W_{adim}(v_g = 0) - v_g$. The frequency and wave-number of the instabilities for a given v_g are then moved back to the static reference frame as follow: $\omega_{static} = \omega(v_g) + \alpha(v_g) * v_g$ and $\alpha_{static} = \alpha(v_g)$. Results of the group velocity sweeping are displayed figure 6. For group velocities under $vg < 0.04$, the saddle S_1 dominates the stability behavior having the largest growth-rate, however, for larger values of v_g a second saddle point noted S_2 for the rest of the study becomes more unstable and leads the stability behavior. The maximum amplification of $\sigma_{max} = 0.45$ is reached for $v_g = 0.16$. Figure 6 also displays the real frequency associated with the corresponding saddle S_2 as a function of v_g, the dimensional frequency reached for $v_g = 0.16$ is $f = 110$ Hz.
If the group velocity is further increased from $v_g = 0.16$, the growth rate of S_1 becomes again greater than the one of S_2. However, looking at the displacement of S_1 and S_2 over the complex wave-number plane as displayed in figure 4, one would see that S_1 moves toward and enters the series of sinks and wells located on the α_i axis and can no longer be considered valid saddle point for the Briggs and Bers criteria.
To asses the nature of the different saddles, the stream-wise velocity and pressure eigenfunctions corresponding to S_1 and S_2 are plotted figure 5 for $v_g = 0.16$.

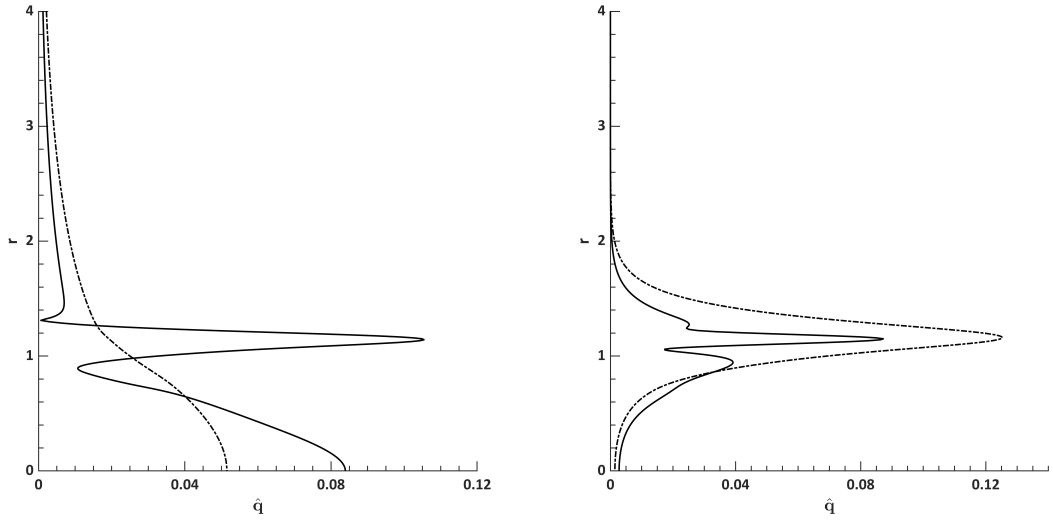

Figure 5: Stream-wise velocity (-) and pressure (- ·) perturbations for saddle points S_1 (left) and S_2 (right), for a group velocity of $v_g = 0.16$, stream-wise position of $z = 1.1$ m in the 100 kW and 150 mbar case.

Eigen-functions associated with the saddle S_1 show that the velocity perturbation occurs both in the outer shear layer of the flow, as well as at the centerline, which is similar to the mode mixed described by Balestra.[1] As for the pressure perturbation, mainly amplified around the centerline, similarly to the jet column modes described by Huerre and Lesshafft.[17] On the other hand, the saddle S_2 displays perturbations shapes typical from the shear layer mode, with no perturbations around the centerline of the jet. The competition mechanism observed in Plasmatron is similar to the one described in top hat jets by Huerre and Lesshafft: at low group velocities, the jet column mode (mixed mode in Plasmatron case) dominate the stability behavior, while at higher group velocities modes of the shear layer type dominate.

3.3 Influence of the stream-wise position

As often stressed in the literature,[8,18] the extent of the absolutely unstable region plays a crucial role in the development and prediction of global instability modes. Therefore, the influence of the stream-wise position in Plasmatron on the stability results is investigated.
A set of discrete positions in the test chamber chosen as $z = [0.7,\ 1.1,\ 2,\ 3]$ m is used to investigate the full impulse response for the 100 kW and 150 mbar case. Furthermore, the saddles S_1 and S_2 introduced in the previous sections are tracked using the local solver from the torch exit at $z = 0.486$ m, down to the end of the test chamber at $z = 3.5$ m. One can note that for accessibility reasons, experimental observations are limited to one metre after the torch exit. A

DOI: 10.13009/EUCASS2019-751

check of the accuracy of the stream-wise tracking of the saddles is done retrospectively to validate the saddles position in the wave-number plane at the set of discrete stream-wise positions, which proved to be accurate up to the order of convergence of the eigenvalues. Results of the full impulse responses are displayed figure 6, while the results of the tracking the absolute growth-rate and frequency of the saddle S_1 are presented in the figures 7 and 8.

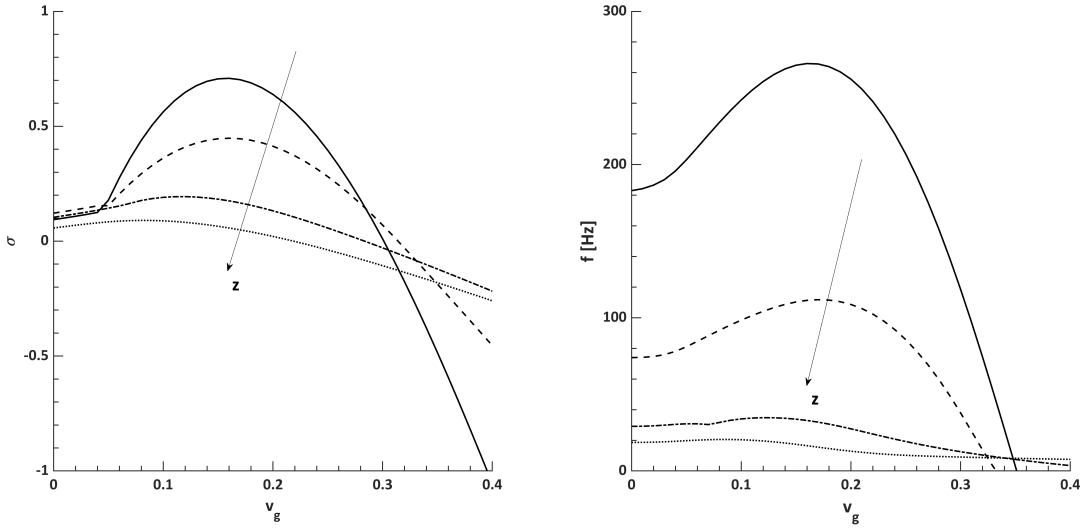

Figure 6: Evolution of the spatio-temporal growth rates σ (left) and real frequency (right) with respect to the group velocity v_g for the stream-wise positions z =0.7 m (-), z =1.1 m (–), z =2 m (-$\cdot$) and z =3 m ($\cdot\ \cdot$) for the 100 kW and 150 kbar case.

The disposition of the growth-rate contours in the wave-number plane is found to remain qualitatively similar for the three first discrete stream-wise positions considered for the full-impulse response. However, for $z = 3$ m, the saddle S_2 is no longer pinched between an α^+ and an α^- branch, but rather between two α^- branches, and thus is no longer valid. Therefore the plot corresponding to z 3 m in the figure 6 is only considering S_1 and no other competition mechanism is found at this position. The shapes of perturbations at the saddle points obtained for the group velocity promoting the largest growth rate $v_g(\sigma_{max})$ is found to remain qualitatively the same for the three first stream-wise positions considered, although expanding in the radial direction as the shear layer gets thicker. However, for the last position $z = 3$ m, saddles seem to exchange their respective shapes at $v_g(\sigma_{max})$: Saddle S_1 displays a pressure perturbation mostly amplified in the shear layer, while the one of S_2 is mostly confined around the centerline of the jet. An interesting result is that for all positions studied, the absolute growth-rate of S_1 at $v_g = 0$ remains positive, indicating that the absolute region extends through the whole test chamber of Plasmatron, which is considerably more than for most cases studied[8] in the literature. This effect is believed to be due to the extreme temperature found in the plasma jet. Saddle S_1 displays a maximum absolute growth-rate of $\sigma_{0,max} = 0.1285$ at $z = 1.2$ m, while remaining marginally positive at the end of the domain. The absolute frequency found at the maximum amplification is $f_0 = 25.7$ Hz. As described by Coenen[8] for jets with non-uniform density layers, a positive slope of the absolute growth rate at the nozzle exit is found for jets where the nozzle diameter is much larger than the shear layer thickness. This is coherent with the results of the stream-wise tracking of saddle S_1, if the outer shear layer due to the annular inlet is considered, rather than the core shear layer of the jet. This is further supported by the shape of the density profiles displayed Figure 2, which display a sharp variation near the outer shear layer, and recalling that the baroclinic torque plays a major role[17] in the promotion of absolute instabilities. The apparent shift between the density and temperature profiles can be further explained by the greater sensitivity of the density to temperature variations for low temperatures when considering a realistic density law, hinting at the importance of taking into account high temperature effects in the base flow computation. Further downstream, the core and secondary streams merge to form a thick shear, and combined with the increase of Reynolds number and temperature ratio $S = T_\infty/T_c$, the absolute growth rate decreases.
On the other hand, the growth-rate of the shear layer modes associated with saddle S_2 are found to reach their maximum value at the exit of the torch, and to decrease along the test chamber. However, for each stream-wise position, the maximum growth rate reached by the convective instability is much larger than the one of the absolute instabilities, similarly to the observations[17] of Lesshafft and Huerre. Additionally the range of dimensional frequencies associated to the convective instabilities is significantly higher than the absolute one.

DOI: 10.13009/EUCASS2019-751

3.4 Influence of the driving parameters

The influence of the facility's driving parameters, namely the static pressure P_s and the electrical power P_{el}, on the stability features of the plasma jet is considered as a generalization of the results obtained in the previous sections. In order to limit the size of the parametric space, the full impulse response is considered in all conditions at a single stream-wise position $z = 1.1$ m corresponding to the area where experimental observations[7] are performed. Once more, the contours of the growth-rate in the complex wave-number plane do not change qualitatively from the one displayed Figure 4. And the same competition mechanism between absolute and convective instabilities is observed. The results of the full impulse response are presented in Table 2 for the conditions studied.

P_{el} (kW)	P_s (mbar)	$v_g\,(\sigma_{max})$	$f_{S2}\,(\sigma_{max})$ (Hz)	σ_{max}
80	100	0.25	180	0.685
80	150	0.23	119	0.644
80	200	0.22	91	0.633
100	100	0.18	169	0.498
100	150	0.16	111	0.448
100	200	0.15	82	0.428
150	100	0.1	130	0.247
150	150	0.1	94	0.216
150	200	0.007	68	0.202

Table 2: Results of the full impulse response for $z = 1.1$ m and different driving parameters of the Plasmatron.

The maximum growth rate σ_{max} is found to be mostly influenced by the variations of the electrical power, while the real frequency at the maximum amplification rather depends mostly on the static pressure. When increasing the power, the maximum growth rate is found to decrease, which is though to be caused by the increase of Reynolds number, and in a lower extent by the increase of Mach number.
The influence of the electric power on the absolute instabilities is also considered, and combined with the influence of the stream-wise position as seen in the Figure 7.

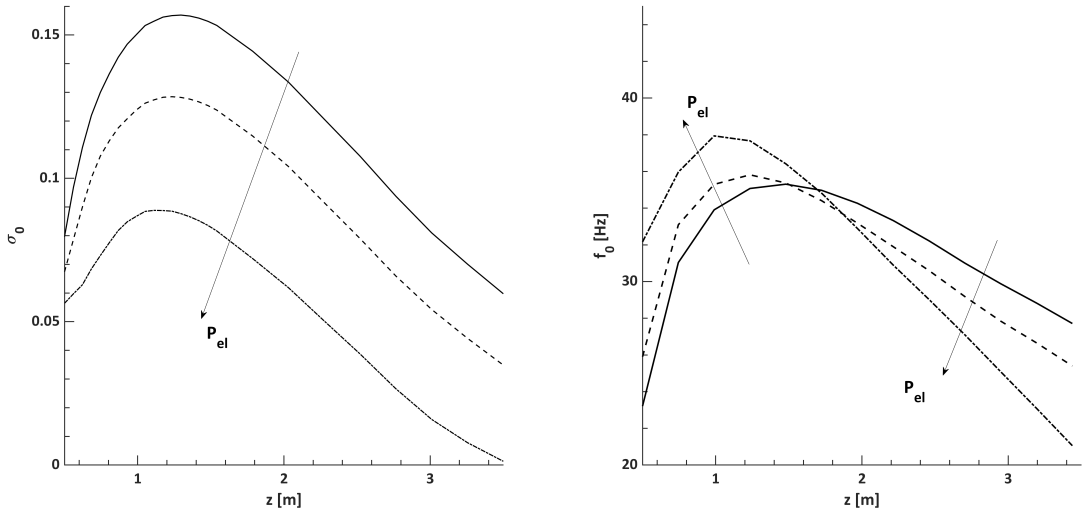

Figure 7: Evolution of the absolute growth rate σ_0 (left) and absolute frequency (right) with respect to the stream-wise position v_g for powers $P_{el} = 80$ kW (-), $P_{el} = 100$ kW (–) and $P_{el} = 150$ kW (- ·).

For the three powers studied, the trend of the absolute growth-rate and frequency is similar to the one described in Section 3.3. However, for $P_{el} = 150$ kW the slope of the growth rate at the torch exit is lower than for the other powers. This observation is consistent with the evolution of the velocity profiles caused by an increase of power: although the bypass ratio decreases, the secondary stream starts to merge the core stream even at the torch exit, and therefore the secondary shear layer found above $r = 1$ becomes slightly thicker. A counter intuitive additional result is that the

DOI: 10.13009/EUCASS2019-751

length at which the absolute growth-rate reaches its maximum value in the chamber seems to scale inversely with the length for which the Reynolds number decreases due to the ionization effect on the viscosity. Therefore the absolute instability characteristics are though to be dependant on the coaxial-nature of the jet and the thickness of the secondary stream shear layer. Similarly to the frequency of the convective instabilities, the sensitivity of the absolute frequency with respect to the electrical power is found to be rather low.

The analysis of the absolute instabilities is also carried out by varying the static pressure of the facility from 100 mbar to 200 mbar while the power is maintained at 100 kW. Results in terms of growth-rate and dimensional frequency are displayed Figure 8.

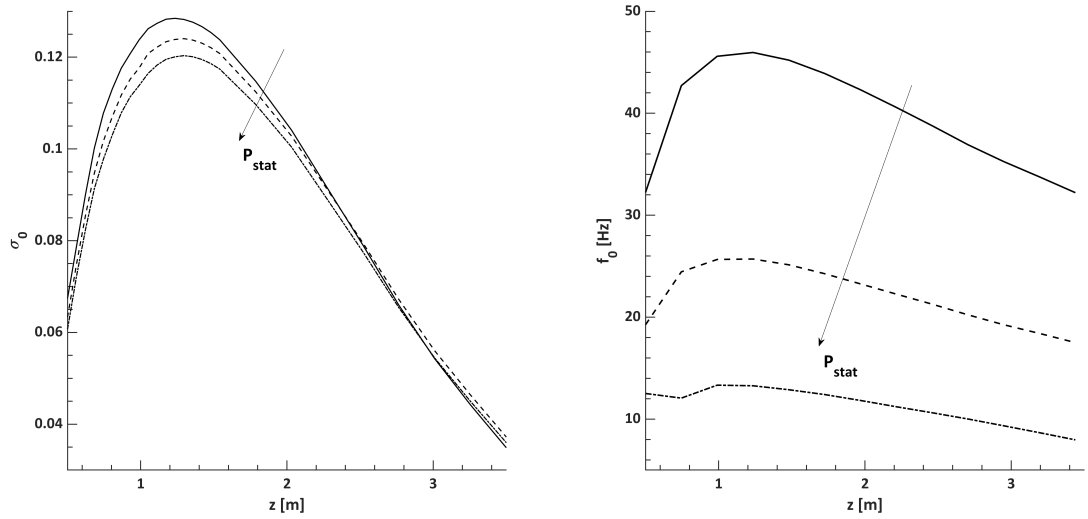

Figure 8: Evolution of the absolute growth rate σ_0 (left) and absolute frequency (right) with respect to the stream-wise position v_g for static pressures P_{stat} = 100 mbar (-), P_{stat} = 150 mbar (–) and P_{stat} = 200 mbar (- ·).

The change of pressure is found to mostly act on the absolute frequencies of the instabilities, while having little influence on the absolute growth-rate. Indeed, when increasing the pressure, the centerline value of the stream-wise velocity is mostly influenced. It is noticed here that the behavior of the absolute frequency f_0 with respect to the pressure is the opposite of the one found for the frequency of the convective instabilities obtained by the full-impulse response. The peak of absolute growth-rate remains in a similar stream-wise position for the different pressures, which is coherent with the small variations of the secondary stream shear layer thickness and bypass ratio observed in the basic state at different pressures.

3.5 Comparison against experimental observations

Experimental observations of Plasmatron jet oscillations are available in the work of Cipullo et al.[7] These results consists in the main oscillation frequencies of the jet obtained by applying fast Fourier Transform (FFT) analysis to high speed camera imaging. The main conclusions of this investigations are that the main frequency of the oscillations decreases for increasing pressures, and increases for increasing powers. Furthermore, pressure is found to be the most influential parameter on the stability behavior, and it is presumed that while varying the pressure, the Strouhal number of the oscillations defined as $St = {}^{fr_0}/_{w_c}$ would remain constant. The main frequencies obtained experimentally are recalled in Table 3, alongside the growth-rate, frequency and corresponding Strouhal numbers of the absolute instabilities found in the present work.

As already mentioned in Section 2.1, this comparison is done assuming a ratio of ½ between the power given to the facility and the power set in CoolFluid-ICP simulations used for the base flow of this study. Therefore, comparison of trends with respect to the power should be regarded with caution.
Values of the absolute instability parameters presented in Table 3 are given for the position corresponding to the torch exit rather than for the locations where the maximum growth rate is reached for the following reason: According to Lesshafft et al.[18] and Coenen,[8] jets displaying a positive absolute growth-rate directly at the nozzle can sustain a global instability modes if the absolute region is long enough, which has been found to be the case for Plasmatron in this

DOI: 10.13009/EUCASS2019-751

P_{el} (kW)	P_s (mbar)	ω_0	f_0 (Hz)	St_0	f_{exp} (Hz)
80	100	0.0825 + 0.0797i	23.25	0.0131	100
80	150	0.0812 + 0.0761i	16.73	0.0129	50
80	200	0.0813 + 0.0747i	13.08	0.0129	50
100	100	0.0646 + 0.0663i	25.59	0.0103	125
100	150	0.0646 + 0.0631i	18.79	0.0103	80
100	200	0.0638 + 0.0607i	14.87	0.0102	50
150	100	0.0513 + 0.0554i	30.72	0.0082	195
150	150	0.0496 + 0.0508i	22.70	0.0079	115
150	200	0.0491 + 0.0485i	18.34	0.0079	77

Table 3: Absolute instability frequency and Strouhal number at the exit of the torch section ($z = 0.5$ m) for Plasmatron's parameters studied.

study. In such situation, the frequency of the global instability is correlated to the value of the local absolute frequency at the nozzle location.
Unfortunately, the range of oscillations frequencies observed experimentally is closer to the values found for the convective instabilities associated with the saddle S_2 in this study, despite the fact that absolute instabilities should dominate the stability behavior of the flow. However, the trends of the absolute frequency with respect to the changes of power and pressure found in this study are in good agreement with the experimental observations, while the frequency behavior of the convective instabilities with respect to the power seems to contradict the experimental results. Although this last point will require a validation of the efficiency of the facility to be verified.
On the other hand, the induction process used to heat the jet is influenced by the alternative nature of the current running through the coils, which imposes a strong forcing on the temperature field. This forcing has been observed experimentally[7] and is especially present at very low pressures. It is therefore conjectured that the observed frequency is the result of a modulation of the global absolute instability mode by the forcing of the coils. This is further supported by the experimental observation of a constant oscillation frequency along the jet[7] after a few diameters from the torch exit.

4. Conclusion

Hydrodynamic instabilities of the jet found in the VKI inductively coupled plasma wind tunnel Plasmatron have been investigated using the spatio-temporal formulation of the Linear Stability Theory and a base flow obtained from multi-physics CFD simulations taking into account high enthalpy effects for a flow in Local Thermo-chemical Equilibrium.
This analysis has shown that the axisymmetric plasma jet sustains a long region of absolute instability bounded by exit of the nozzle for all the conditions studied. Which is coherent with the literature and the extreme values of the temperature ratio in the jet. The nature of the absolute instabilities has been correlated to the jet column/shear mixed modes also observed by Balestra[1] and Gloor[11] in co-flow jets. This mode displays a strong amplification of the stream-wise perturbation at the centerline and in the secondary stream of the jet caused by the annular inlet of Plasmatron. The full impulse response of the flow has been studied by varying the group velocity. By doing so, a competition mechanism between the absolute mixed outer and a convective shear layer mode has been identified, similar to the one observed by Huerre and Lesshafft in[17] in heated jets. The evolution of the absolute instability parameters showed a region with a positive slope of the absolute growth rate at the beginning of the test chamber, while convective instabilities were found to only decrease with the stream-wise position. A parametric study of the instabilities has been performed by varying the facility's power and pressure, highlighting the dependence of the absolute instability region to the shear layer thickness of the secondary stream. Such results are also coherent with the role of the the baroclinic torque occurring with the alignment of a region of strong density variations with the outer shear layer. For both absolute and convective instabilities, the growth rate is found to depend mainly on the power, while the frequency depends mainly on the pressure. A comparison of the frequencies found with LST against experimental observations of Cipullo[7] showed a good agreement when considering the trends of absolute frequency against the jet oscillations. As predicted by Cipullo et al., the Strouhal number based on the absolute frequency at the torch's exit has been found to be constant with respect to pressure variations. Finally a possible interpretation of the mismatch between the frequency values found with LST and experimentally was proposed.

DOI: 10.13009/EUCASS2019-751

5. Acknowledgments

This work benefited from the discussions with F. Mirò Mirò from the Von Karman Institute and with U. Ali Qadriis from Cambridge University and is supported by the Fonds de la Recherche Scientifique - FNRS under the FRIA Grant.

Appendix

Analytical fitting for basic state

The analytical fitting of the CFD velocity and temperature profiles are done for a set of discrete stream-wise positions using the following expressions:

$$\begin{aligned} W_{adim}(r) = a_w * GN(r, 0, b_w) + c_w(1 - tanh(d_w(r - e_w))) \\ + f_w(1 - tanh(g_w(r - h_w))) * GN(r, i_w, j_w) * r^2, \end{aligned} \tag{3}$$

$$\begin{aligned} T_{fit}(r) = a_T * GN(r, 0, b_T) + c_T(1 - tanh(d_T(r - e_T))) \\ + f_T(1 - tanh(g_T(r - h_T))) + i_T(1 - tanh(j_T(r - k_T))), \end{aligned} \tag{4}$$

Where $r = \frac{r_{dim}}{L_{ref}}$, and GN is the Gaussian function defined as:

$$GN(r, a, b) = \frac{1}{(b\sqrt{2\pi})} exp(\frac{(-(r - a)^2}{2b^2}) \tag{5}$$

The temperature profiles are then shifted to take into account the finite temperature in the outer flow of the test chamber set to $T_\infty = 350$ K as:

$$T_{adim}(r) = (T_{fit}(T_c - T_\infty) + T_\infty)/T_c \tag{6}$$

Where T_c is the local value of the centerline temperature obtained from the CFD. The value of the coefficients are determined using MATLAB^{TM} *fit* routine.

References

[1] G. Balestra, M. Gloor, and L. Kleiser. Absolute and convective instabilities of heated coaxial jet flow. *Physics of Fluids*, 27(5):054101, 2015.

[2] A. Bayliss and E. Turkel. Mappings and accuracy for Chebyshev pseudo-spectral approximations. *Journal of Computational Physics*, 101(2):349–359, 1992.

[3] A. Bers. Space-time evolution of plasma instabilities-absolute and convective. In *Basic plasma physics*, page 451, 1984.

[4] B. Bottin, M. Carbonaro, V. Van Der Haegen, A. Novelli, and D. Vennemann. The VKI 1.2 MW Plasmatron facility for the thermal testing of TPS materials. *3 rd European Workshop on Thermal Protection Systems, ESTEC,*, 1998.

[5] R. J. Briggs. *Electron-stream interaction with plasmas*. M.I.T. Press, Cambridge, 1964. OCLC: 537479.

[6] M. Chiatto. Numerical study of plasma jets by means of linear stability theory, 2014.

[7] A. Cipullo, B. Helber, F. Panerai, F. Zeni, and O. Chazot. Investigation of freestream plasma flow produced by inductively coupled plasma wind tunnel. *Journal of Thermophysics and Heat Transfer*, 28(3):381–393, 2014.

[8] W. Coenen and A. Sevilla. The structure of the absolutely unstable regions in the near field of low-density jets. 713:123–149.

[9] A. Dorsa. Energy balance for plasmatron facility, 2015.

[10] F. Garcia Rubio. Numerical study of plasma jet unsteadiness for re-entry simulation in ground based facilities, 2013.

DOI: 10.13009/EUCASS2019-751

[11] M. Gloor, D. Obrist, and L. Kleiser. Linear stability and acoustic characteristics of compressible, viscous, subsonic coaxial jet flow. *Physics of Fluids*, 25(8):084102, 2013.

[12] K. J. Groot, F. Miro Miro, E. S. Beyak, A.J. Moyes, F. Pinna, and H. L. Reed. Dekaf: Spectral multi-regime basic-state solver for boundary-layer stability. *2018 Fluid Dynamics, Conference, AIAA AVIATION Forum, (AIAA 2018-3380)*, 2018.

[13] P. Huerre and P. A. Monkewitz. Absolute and convective instabilities in free shear layers. *Journal of Fluid Mechanics*, 159:151–168, 1985.

[14] M. P. Juniper. The effect of confinement on the stability of non-swirling round jet/wake flows. *Journal of Fluid Mechanics*, 605:227–252, 2008.

[15] N. Kumar. Spatio temporal stability of shear layers. *S.T. report, von Karman Institute*, 2017.

[16] A Lani. An object oriented and high performance platform for aerothermodynamics simulation. *Ph.D. thesis, von Karman Institute/Universite Libre de Bruxelles*, 2008.

[17] L. Lesshafft and P. Huerre. Linear impulse response in hot round jets. *Physics of Fluids*, 19(2):024102, 2007.

[18] Lutz Lesshafft, Patrick Huerre, and Pierre Sagaut. Frequency selection in globally unstable round jets. *Physics of Fluids*, 19(5):054108, May 2007.

[19] A. Michalke. Survey on jet instability theory. *Progress in Aerospace Sciences*, 21:159–199, 1984.

[20] F. Miro Miro, E. S. Beyak, F. Pinna, and H. L. Reed. High-enthalpy models for boundary-layer stability and transition. 31(4):044101.

[21] P. Monkewitz and K. Sohn. Absolute instability in hot jets and their control. In *10th Aeroacoustics Conference*, Seattle, WA, U.S.A., 1986.

[22] P. A. Monkewitz, D. W. Bechert, B. Barsikow, and B. Lehmann. Self-excited oscillations and mixing in a heated round jet. *Journal of Fluid Mechanics*, 213:611–639, 1990.

[23] F. Pinna. *Numerical Study of Stability Fo Flows from Low to High Mach Number*. Von Karman Institute for fluid dynamics, 2012.

[24] F. Pinna and K. Groot. Automatic derivation of stability equations in arbitrary coordinates and for different flow regimes. In *44th AIAA Fluid Dynamics Conference*, AIAA AVIATION Forum. American Institute of Aeronautics and Astronautics.

[25] J. B. Scoggins and T. E. Magin. Development of mutation++: Multicomponent thermodynamics and transport properties for ionized gases library in c++. *11th AIAA/ASME Joint Thermophysics and Heat Transfer Conference, AIAA AVIATION Forum, (AIAA 2014-2966)*, 2014.